January 2002 • NREL/CP-500-30917

Conference Paper

The NREL Large-Scale Turbine Inflow and Response Experiment — Preliminary Results

Preprint

N. Kelley, M. Hand, S. Larwood, and E. McKenna

To be presented at the 21st American Society of Mechanical Engineers Wind Energy Symposium
Reno, Nevada
January 14–17, 2002

National Renewable Energy Laboratory

1617 Cole Boulevard
Golden, Colorado 80401-3393

NREL is a U.S. Department of Energy Laboratory
Operated by Midwest Research Institute • Battelle • Bechtel

Contract No. DE-AC36-99-GO10337

THE NREL LARGE-SCALE TURBINE INFLOW AND RESPONSE EXPERIMENT – PRELIMINARY RESULTS

Neil Kelley
Maureen Hand
Scott Larwood
Ed McKenna

National Wind Technology Center
National Renewable Energy Laboratory
Golden, Colorado

ABSTRACT

The accurate numerical dynamic simulation of new large-scale wind turbine designs operating over a wide range of inflow environments is critical because it is usually impractical to test prototypes in a variety of locations. Large turbines operate in a region of the atmospheric boundary layer that currently may not be adequately simulated by present turbulence codes. In this paper, we discuss the development and use of a 42-m (137-ft) planar array of five, high-resolution sonic anemometers upwind of a 600-kW wind turbine at the National Wind Technology Center (NWTC). The objective of this experiment is to obtain simultaneously collected turbulence information from the inflow array and the corresponding structural response of the turbine. The turbulence information will be used for comparison with that predicted by currently available codes and establish any systematic differences. These results will be used to improve the performance of the turbulence simulations. The sensitivities of key elements of the turbine aeroelastic and structural response to a range of turbulence-scaling parameters will be established for comparisons with other turbines and operating environments. In this paper, we present an overview of the experiment, and offer examples of two observed cases of inflow characteristics and turbine response collected under daytime and nighttime conditions, and compare their turbulence properties with predictions. *

* This work was performed at the National Renewable Energy Laboratory in support of the U.S. Department of Energy under contract number DC-AC36-98-GO10337.

INTRODUCTION

Experience with the large, multi-megawatt prototype wind turbines in the late 1970s and early 1980s revealed the structural loads experienced by these machines significantly exceeded predicted levels. In some cases, this contributed to operating lifetimes much shorter than expected. Closer examination of these predictions showed that the excess loads were directly attributable to the impact of atmospheric turbulence encountered by the turbine rotor blades. In 1988, an effort within the Federal Wind Program established goals to develop (1) a physical understanding of the role of inflow turbulence in the structural response of wind turbines, and (2) numerical simulations of this turbulence that incorporate those properties of the flow that have significant influence in the dynamic response of wind turbines and can serve as the excitation for structural design codes. Both of these objectives are critical in the development of efficient, reliable wind turbines with long operating lifetimes.

Previous Work

In 1988, Veers[1] demonstrated the importance of the stochastic turbulent wind through the use of a numerical simulation of only the streamwise wind component spatially across a rotor disk in a neutral (adiabatic) atmosphere. Through the analysis of the combined turbulence and turbine response based on measurements made in a very large, 41-row wind farm in San Gorgonio Pass, California, Kelley[2,3,4] established the correlation of atmospheric stability and the spatial variation of the three-dimensional inflow wind vector; e.g., the crosswind and vertical wind components as well as the streamwise component, in inducing large structural loading events. Sutherland and Kelley[5] used the observed structural response data to demonstrate that turbulence conditions within a closely-spaced, multi-row wind farm induce higher levels of fatigue damage than occur in the equivalent of individual

turbines operating in relatively uniform terrain. Kelley[6] expanded Veers' original turbulence simulation code (called SNLWIND) to include all three turbulent wind components using spectral and cross-correlation models tailored to the environment upwind, downwind, and within the San Gorgonio wind farm environment as well as over flat, uniform terrain. He called this expanded code SNLWIND-3D. Kelley et al.[7] and Kelley and Sutherland[8] used this code to simulate a full diurnal inflow variation seen upwind and downwind of the San Gorgonio wind farm for two turbine designs using three different design codes of varying capability. The predicted load spectra agreed reasonably well with observations, though discrepancies between the measured and predicted fatigue damage were more pronounced.

Using the San Gorgonio wind farm measurements and those from testing a very flexible turbine at the National Wind Technology Center (NWTC) Kelley et al.[9,10] applied wavelet analysis to expand the details of the turbulence/rotor interaction. This technique allows the examination of short-period loading events in terms of the turbulent inflow and structural response in the frequency domain. The results clearly demonstrate that large, damaging load events in turbine rotors occur when the blades pass through organized or coherent patches of turbulence. The results also explain the higher fatigue damage accumulations within closely spaced, multi-row wind farms because of the increased presence of higher levels of coherent turbulence (particularly at night) than is seen where there are no turbines operating upstream. Thus wind turbines must be carefully designed if they are destined to operate in wind farm conditions or in regions of the earth's atmospheric boundary layer where energetic, coherent turbulence is known to exist a significant percentage of the turbine operating time.

The LIST Program

In 1999 the Long-term Inflow and Structural Testing Program (LIST) was established to obtain the necessary measurements to answer several questions that have been barriers to further progress in meeting the goals stated earlier. In particular questions related to the inflow translated into the following objectives:

- Compare measured spatial inflow properties important to wind turbine operations with those simulated with the SNLWIND-3D turbulence code, and establish any systematic differences as a function of boundary-layer conditions
- Establish whether or not it is possible to modify the present formulation of the SNLWIND-3D code to bring the simulated properties into closer agreement with observations obtained by LIST field measurements up to heights of 60 m or more above the ground
- Establish sensitivities of turbine aeroelastic and structural response to a range of turbulence-scaling parameters and compare with other turbines and operating environments.

In the summer of 2000, a capability was established at the NWTC to meet at least some of these objectives. A 42-m (137-ft) planar array consisting of five high-resolution sonic anemometers and supporting meteorological instrumentation was installed 1.5 rotor diameters upwind of the 42-m diameter, 600-kW NWTC Advanced Research Turbine (ART). A limited number of aeroelastic, structural, and supporting measurements were provided on the ART. Precision timing derived from the satellite-based Global Positioning System (GPS) was used to synchronize the inflow and turbine-based measurements recorded on separate data acquisition systems. Data was collected during the NWTC primary wind season from October 28, 2000, to May 17, 2001.

In this paper we briefly discuss the NWTC LIST experimental configuration used to measure the turbine inflow and the measurements on the turbine itself. We present two cases from the LIST data set that, we believe, exemplify many of the issues that need to be addressed. Finally we present some of our initial conclusions and briefly discuss our future activities in analyzing this new information and follow-up field experimentation.

TURBULENCE SCALING

The planetary boundary layer (PBL) of the earth's atmosphere can be divided into at least three regions or vertical layers. The upper two, the surface and mixed layers, are important to wind turbines.

Surface Layer

The surface layer, strictly speaking, is only defined for flows over flat, homogenous terrain. Under some conditions, it may not even exist. The turbulence structure within this layer is amenable to scaling by a relatively small number of parameters**.** Turbulence in the surface layer is characterized by a near-constant vertical flux of momentum with height and by a positive (upward) heat flux during the day and negative (downward) flux at night. The vertical flux of turbulent kinetic energy (TKE) is positive; i.e., away from the surface due to friction. The daytime or convective surface layer is considerably different

than its nighttime or nocturnal counterpart. During the unstable daytime hours, the turbulent eddies are very large, but at night, under stable conditions, they tend to be much smaller and more coherent or organized because of the retardation of vertical motions by the negative buoyancy. The daytime surface layer is usually much deeper. Under strong surface heating, this layer can often extend up to 10% of the entire boundary-layer depth, or 100 to 150 m. The nocturnal or stable surface layer is usually much thinner, ranging from 10 to 50 m, depending on the strength of the wind and cloud cover conditions. Thus wind turbines whose rotors operate either partly or completely above about 50 m will experience turbulence, the structural properties of which may not be adequately simulated by currently available simulation codes, particularly at night.

Mixed-Layer

The region between the upper limits of the surface layer and the top of the PBL is called the *mixed layer*. The flow dynamics of this layer are quite different from those that dominate the surface layer and therefore follow other turbulence-scaling relationships. For example, the influence of the earth's rotation (Coriolis force) can be ignored in the surface layer but not in the mixed layer. The daytime mixed layer is also dominated by large-scale convective circulations whose strengths are influenced primarily by heat rising from the surface (vertical heat flux) and the depth of the PBL. The influence of the ground is minimal. The thermal field is much more important in the mixed layer.

The stable, or nocturnal mixed layer, is often characterized by its independence of what is happening at the surface; i.e., flow conditions here are decoupled from those below. The formation and evolution of nocturnal low-level jet streams is a good example. Here the flow near the surface becomes retarded as the ground cools, and eventually the stronger winds aloft suddenly overshoot and accelerate under the influence of only the pressure gradient and Coriolis forces initiating the jet evolution. The nocturnal mixed layer is often strongly stratified with height, as evidenced by the large vertical gradients of wind speed and temperature. Locally these gradients can be responsible for the development of internal gravity waves and Kelvin-Helmholtz instabilities that serve as the source of intense, coherent turbulent structures when they form, propagate, and decay. The region immediately below the peak wind speeds of the low-level jet is particularly well suited to the generation of atmospheric wave motions. There is no clear consensus on turbulence scaling in the nocturnal mixed layer because often the background turbulence is low and unorganized but punctuated by brief bursts of intense, coherent turbulent motions.

EXPERIMENTAL OVERVIEW

The experiment was conducted at the National Renewable Energy Laboratory's (NREL) NWTC, which is located downwind of the Front Range of the Colorado Rocky Mountains and about 40 km (25 mi) northwest of Denver, Colorado. While the terrain becomes quite complex several kilometers to the west of the NWTC, it is locally quite homogenous immediately upwind of the test turbine, rising only on the order of 25-30 m over an upwind horizontal distance of 2 km. The ART test turbine is located near the easternmost boundary of the NWTC property. The winds at the NWTC are predominately from the west to west-northwest. Strong downslope winds are common during the primary wind season of October through May. Banta et al.[11], using high-resolution Doppler lidar measurements, documented the existence of nocturnal low-level jet streams passing over the NWTC that originate as outflows from steep-walled Eldorado Canyon to the west-northwest. Figure 1 displays the turbine, measurement array, and upstream topography in the direction of the prevailing wind. Eldorado Canyon is in the background to the right of the turbine tower.
The experiment was designed to measure the turbulent inflow in a plane immediately upwind of

Figure 1. NWTC LIST 42-m inflow measurement array upwind of ART turbine and looking towards prevailing wind direction

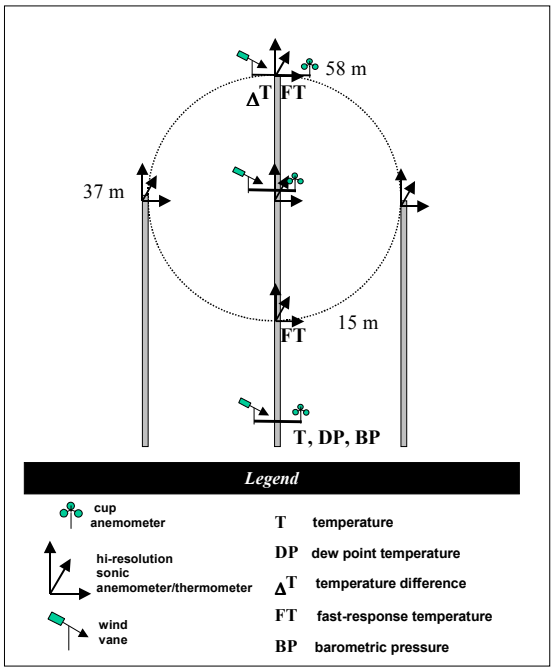

Figure 2. Schematic of NWTC LIST inflow measurement array instrumentation deployment

the 42-m (137-ft) diameter turbine rotor and the corresponding response of key turbine structural parameters. The inflow instrumentation consisted of a planar array of anemometry, temperature, and moisture measurements installed 1.5-rotor diameters upstream of the turbine rotor. Turbine response measurements were made with a combination of strain gauges, accelerometers, and rate gyroscopes in addition to the operational measurements of blade pitch, teeter, and yaw angles, and generator power. Each set of measurements was recorded by its own data acquisition system along with a common high-resolution time base derived from the GPS to allow each data set to be synchronized during post processing. Following is a brief discussion of the details of the inflow and turbine measurement systems.

Inflow Measurements

The inflow instrumentation was mounted on three towers located 1.5-rotor diameters upstream of the turbine rotor. A total of five high-resolution Kaijo Model DA-600 ultrasonic anemometers/thermometers, which have a 10-Hz data bandwidth and a minimum resolution of 0.005 m/s or less, were deployed. In addition, cup anemometers and wind vanes were installed on the 61-m central tower at three levels, along with air temperature, fast-response temperature, temperature difference between 3 and 61 m, and dew point temperature sensors. Barometric pressure was measured at a height of 3 m. GPS-based time was recorded to a resolution of 1 millisecond. The raw data was collected at rate of 40 samples per second. A schematic of the inflow measurement array is shown in Figure 2.

There was a concern for the amount of movement of the sonic anemometers at the end of the 3.5-m (11.5-ft) support arms installed on the central tower under high wind loads. We were worried about the possibility of having motions within the frequency range of the sonic anemometers and corrupting the integrity of the velocity measurements. Three steps were taken to minimize induced motions. The first was to install a guying system that incorporated two torque arms to increase the torsional stiffness of the tower as much as possible. The second step was to develop a dynamics model of the tower to assess the maximum response amplitudes of the instrument supports and tower combination at frequencies within the sonic measurement range.[12] This was done and the model was excited with a simulated strong, turbulent wind with a mean wind speed of 30 m/s (67 mph) at the 37-m (121-ft) elevation. This was statistically similar to that which could be expected at the NWTC. It was found that, under such conditions, the support velocities in the frequency range of interest would likely exceed the acceptable minimum of 0.1 m/s. As a result, three-axis, ±2g force-balance accelerometers were attached to each sonic anemometer in order to remove tower-motion induced velocities above the allowable minimum of 0.1 m/s using velocities derived from the integrated measured accelerations during the post processing of the data. Finally, special support arms were designed and constructed that damped motions in the support over the 0-10 Hz range, leaving the only uncontrolled motions originating from the tower itself[12]

During post processing, no corrections were made to the sonic-derived velocities of an individual 10-minute record unless one of the peak mount velocities exceeded 0.1 m/s. We have found this occurred in only a very few of more than 7000 records. One in particular was during the period when the highest peak gust of 45.9 m/s (103 mph) was recorded within the array on April 7, 2001, between 02:10 and 02:20 local standard time (LST). The 10-minute mean hub wind speed was 29.5 m/s (69 mph). Histograms of the instantaneous support velocities parallel to the support arm (V_x), lateral to the arm (V_y), and vertical (V_z) for the 15-, 37-, and 58-m (49-, 121-, and 190-ft) elevations are plotted in Figure 3 for this record. It is clear that the induced velocities in the sonic anemometer signals were held

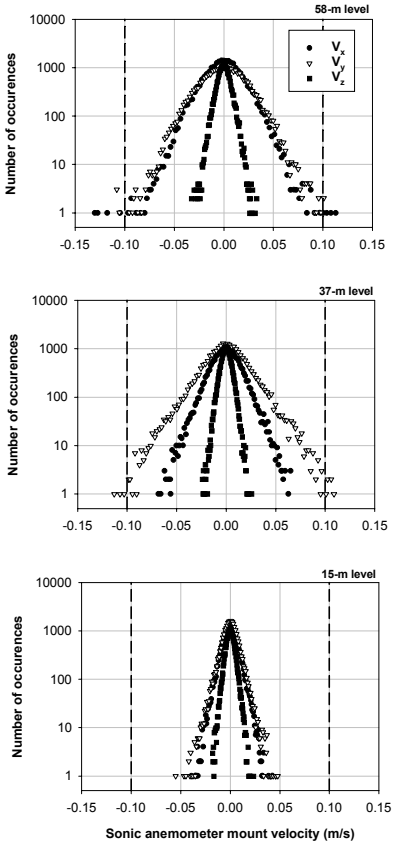

Figure 3. Frequency distributions of sonic anemometer support velocities for 15-, 37-, and 58-m heights on central tower

within acceptable limits (< 0.1 m/s), even under these extreme conditions, when only a few samples were observed outside the desired maximum.

The data was recorded in 16-bit accuracy by a PC-based, real-time data acquisition system using National Instruments interfacing electronics and LabView® software[13]. Two acquisition modes were used. One started and stopped the recording (after completing a 10-minute record) when a discrete signal from the turbine data acquisition system indicated the turbine was operating and it was collecting data. The other started and stopped recording based on operator furnished time limits and independent of the state of the turbine. The latter was often used when wind speeds above the turbine cutout velocity were expected in order to capture the details of high-wind events. The discrete signal indicating that turbine data was being collected is also included in the recorded information. A total of 7035 10-minute inflow records were collected. An extensive post processing of the raw data was performed to place the turbulence information in the proper coordinate system for analysis and interpretation. A comprehensive database consisting of time series and statistical summaries has been developed.

Turbine Measurements

The ART turbine was used as a sensor to help interpret the impacts of the inflow turbulence structure on operating wind turbines. The ART is a 600-kW, two-bladed upwind machine with a teetered 42-m (137-ft) rotor diameter and a hub height of 37 m (121 ft). Full-span pitch control is used to modulate peak power at constant rotor rotational speed of 43 rpm. The turbine cut-in and cutout wind speeds are approximately 6 and 22 m/s (13 and 49 mph), respectively.

Strain gauges were used to measure flapwise and edgewise root-bending moments on each blade and low-speed shaft torque. Absolute digital encoders were used to measure the blade pitch, rotor teeter, and nacelle yaw angles. Generator power was also measured. An inertial measurement unit (IMU) consisting of an orthogonal triad of ±2g force-balance accelerometers and three ±100 deg/s rate gyroscopes was mounted on the forward low-speed shaft support bearing housing immediately behind the rotor. The sensitive axes of the accelerometers were aligned in a right-handed coordinate system with the *X*-axis parallel to the low-speed shaft, the *Y*-axis lateral to it, and the *Z*-axis vertical. The rate gyros measured the angular rotation rate about each of these axes or Ω_x (roll), Ω_y (pitch), and Ω_z (yaw). During post processing, the zero-mean accelerations were integrated both singly and doubly to obtain velocities and displacements along the *X*, *Y*, and *Z* axes.

A pulse-code-modulation (PCM) digital data acquisition system was used to store the turbine measurements and ancillary information. This system was originally developed for the NREL Unsteady Aerodynamics Experiment described by Simms[14]. Two PCM streams collected measurements in the rotating and non-rotating frames respectively with 12-bit conversion resolution and a native sampling rate of 500 samples per second. Six-pole, low-pass Butterworth filters with 20 Hz cut-off frequencies were provided on all of the analog channels. A GPS receiver and time base was incorporated into one of the PCM streams to provide time synchronization with the inflow recording system. A PC-based real-time acquisition program decimated the sampling rate to 80 samples per second after the PCM streams were decommutated and prior to storage on the computer hard disk drive. A total of 3549 10-minute records were collected for analysis.

This number is about half of the available inflow records because often the winds were above the turbine cut-out speed and at other times the inflow system was run in synchronization with data being collected on the NWTC 82-m (270-ft) site meteorological tower in order to gather spatial information. During the last step of the post processing, the sample rate was further reduced to 40 samples per second to allow precise time synchronization with the corresponding inflow data stream. A comprehensive database consisting of time series and statistical summaries of the turbine measurements has been developed.

EXAMPLE CASES

To illustrate the relationship between atmospheric stability and wind turbine load conditions, two 30-minute wind conditions were selected from the LIST database. Both conditions had similar mean hub-height wind speeds and wind directions, but atmospheric stability, turbulence intensity, and friction velocity within the layer occupied by the turbine differed between the two cases, as shown in Table 1. The nocturnal, stable case (Ri > 0) occurred on February 5, 2000, at about 22:00 LST, while the daytime, unstable case (Ri < 0) occurred on March 1, 2000, at about 10:00 LST.

Table 1. Inflow Statistics for Two Example Cases

	Daytime (unstable)	Nocturnal (stable)
Hub mean wind speed (m/s)	13.6	13.7
Hub mean wind direction (deg)	283	287
Turbine layer gradient Richardson number, *Ri*	−0.056	+0.016
Hub turbulence intensity	15%	25%
Rotor disk power law exponent	0.098	0.142
Hub Friction velocity, u_* (m/s)	0.722	1.140

For comparison with inflow measurements, the SNLWIND-3D turbulence simulation code was run using three of the available turbulence models for both of the above inflow cases. The eddy velocity component cross-correlation coefficients of the SMOOTH terrain and upwind wind farm (WFUPW) models were perturbed until the three mean, hub-height Reynolds stresses for each simulation were within 5% of those of the measured values for each inflow case. The mean Reynolds stresses are turbulent flow properties defined as the covariances $\overline{u'w'}$, $\overline{u'v'}$, and $\overline{v'w'}$, where *u', v',* and *w'* are the streamwise, crosswind or lateral, and vertical eddy or perturbation velocity components, respectively, This feature is not available in the IEC Kaimal (IECKAI) turbulence model because in the IEC definition, the Reynolds stresses are not dealt with explicitly. It uses only bulk statistics, such as the mean wind speed and a definition of the turbulence level as boundary conditions.

The logarithmic spectra for the measured hub-height turbulence components as well as for those predicted by each of the three turbulence models are compared for both the daytime and nocturnal boundary layer cases in Figure 4. There is reasonable agreement between the observed and predicted streamwise or *u'* velocity component spectra for both cases. However, there is more energy present in the observed lateral component spectra (*v'* and *w'*) at low frequencies (longer wavelengths) than is predicted by any of the models. The high-frequency (shorter wavelengths) portion of the daytime IECKAI spectra shows higher energies than either that observed or predicted by the SMOOTH or WFUPW models (which are in close agreement). This is a consequence of the IECKAI assuming neutral stability conditions while the actual flow is unstable.

In Figure 5 we compare the observed and predicted logarithmic spectra of the corresponding three *instantaneous* Reynolds stress components; i.e., *u'w'*, *u'v'*, and *v'w'*. As is the case with the eddy components, there is reasonable agreement between the observed and simulated *u'w'* stress component spectra for the unstable daytime case. The low-frequency contributions for the *u'v'* and *v'w'* stress components tend to be underestimated by the simulations, particularly for the latter. Again, the high-frequency range of the IECKAI stress spectra are overstated due to the neutral stability specification. For the stable nocturnal case, there is considerable disagreement between all three of the observed and simulated stress components at frequencies below about 0.5 Hz. The measured stress spectra indicate that there are considerably higher levels of coherent turbulent energy occurring at periods longer than about 2 seconds. The greatest discrepancy is with the *u'w'* and *v'w'* stress components predicted by the IECKAI simulation. However, there is reasonably good agreement at higher frequencies.

The temporal behavior of the inflow Reynolds stress field can be more closely examined using probability density distributions for each of the three instantaneous Reynolds stress components. These are presented in Figure 6. Being consistent with its neutral stability, the IEC turbulence model over

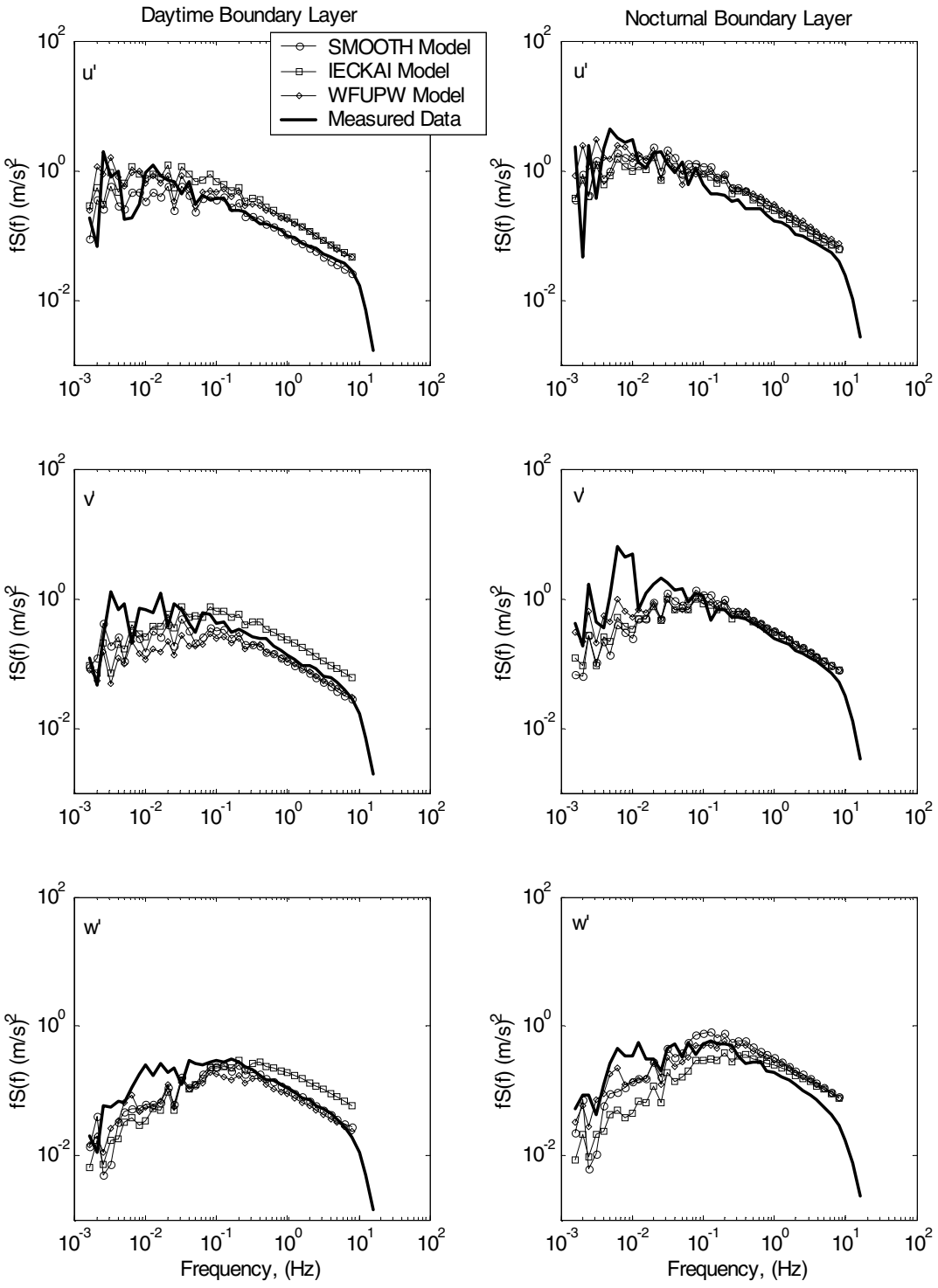

Figure 4. Measured and predicted spectra of 37-m (hub) height eddy wind components for daytime and nocturnal boundary layer example cases

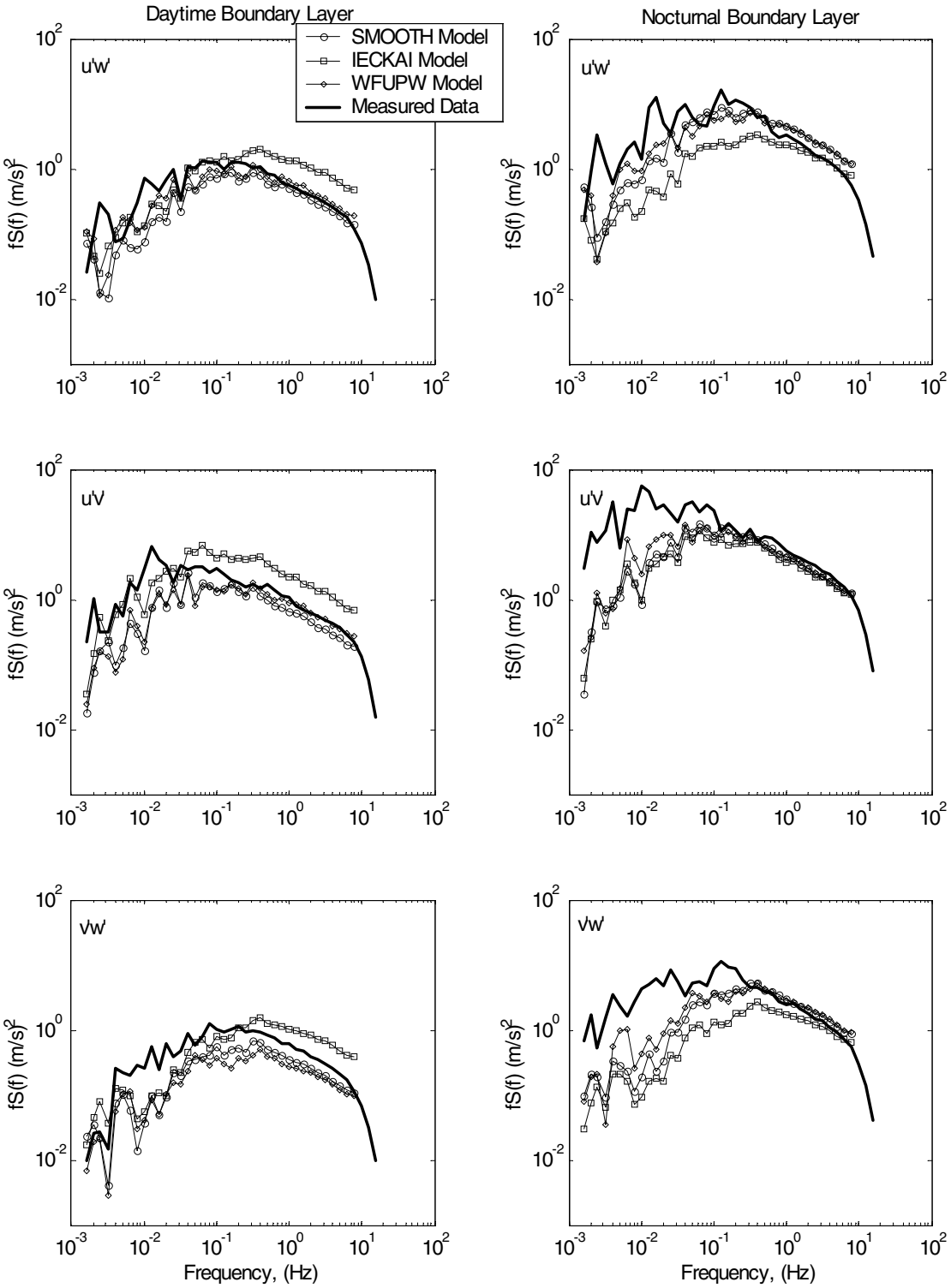

Figure 5. Measured and predicted spectra of 37-m (hub) height instantaneous Reynolds stress components for daytime and nocturnal boundary layer example cases

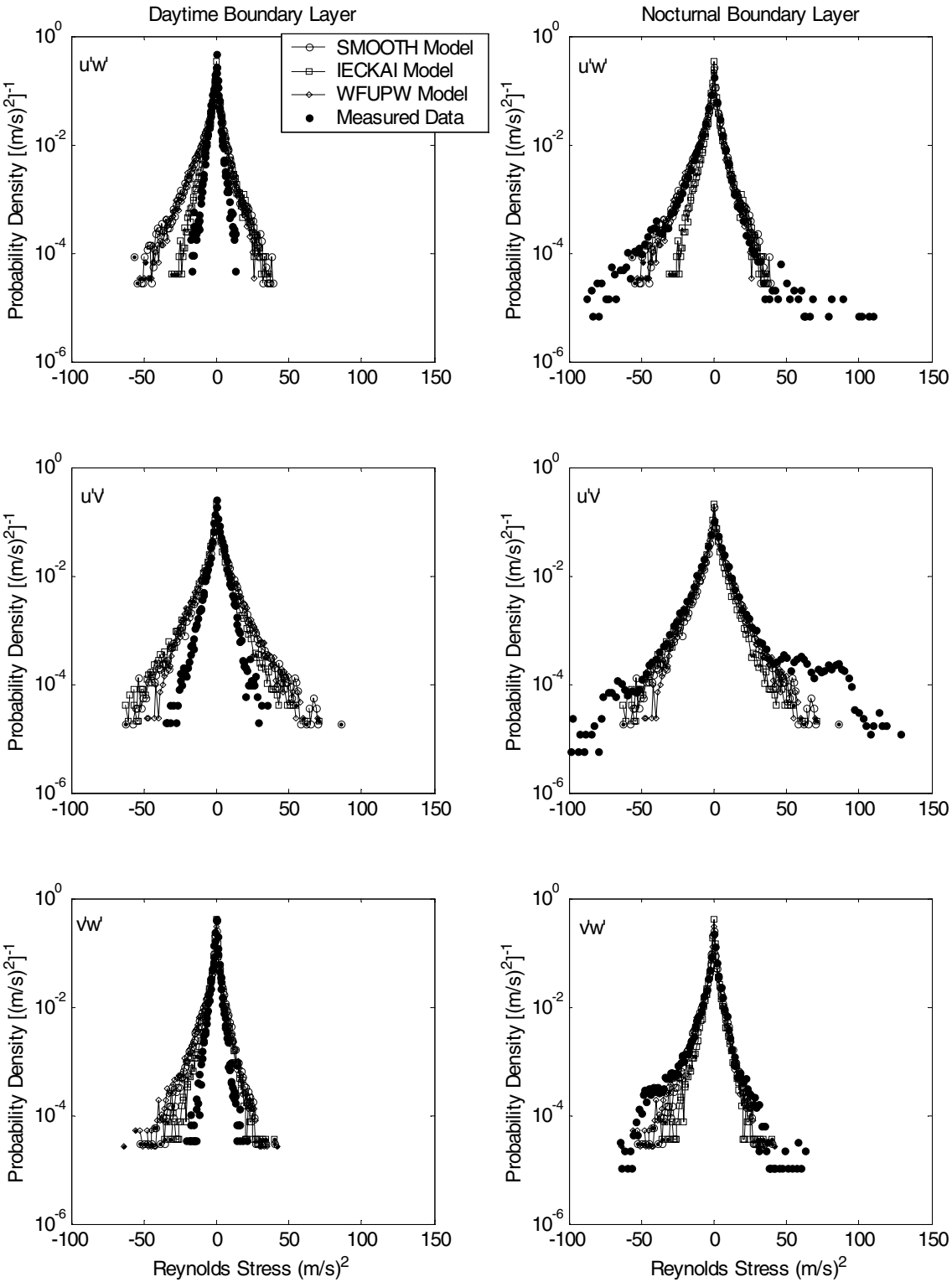

Figure 6. Probability density distributions of measured and predicted instantaneous Reynolds stress components for daytime and nocturnal boundary layer example cases

predicts the maximum Reynolds stresses relative to the other predictions and observed data for the daytime boundary layer. With the exception of the *u'v'* stress component, the smooth terrain and upwind wind farm model predictions agree quite well with observations. In the nocturnal boundary layer case, the smooth terrain and wind farm models perform better than the IEC model in matching the magnitudes of the measured Reynolds stress components. However, the extreme measured Reynolds stresses (distribution tails) are not adequately simulated by any of the three models.

The occurrence of the extreme magnitude Reynolds stresses is concentrated in one segment of approximately 30 seconds within the 30-minute nocturnal (stable) boundary layer record. A 10-minute time series of Reynolds stresses containing these extreme values is shown in Figure 7(b) and are associated with the strong wind gust shown in Figure 7(a) near 500 seconds into the record. The burst of high levels of the instantaneous Reynolds stresses and turbulent kinetic energy or TKE = e = $1/2\left(u'^2+v'^2+w'^2\right)$ in Figure 7(c) indicates the presence of an intense coherent turbulent structure at the turbine hub height. Table 2 shows the maximum and minimum values for the inertial measurement unit (IMU) angular rate and displacement measurements over each of the three individual 10-minute records included within the total 30-minute record (30-minute maxima and minima are shaded).

Typically, the extremes associated with the nocturnal, stable case are twice those seen during the daytime case. These extreme values occurred within the record near the coherent turbulent structure near 500 seconds as illustrated in Figures 7(d-f). Only the maximum roll angle rate occurred later in the record. The magnitude of these excursions is generally higher during the nocturnal case. During this event, the root of the blade experienced a flapwise load cycle of 560 kNm (+300 to −260 kNm) over a period of 10-12 seconds. A 10-minute time series for daytime conditions is shown in Figure 8 for comparison. Noteworthy is the absence of turbulent burst events and associated turbine IMU parameter response seen in Figure 7. The corresponding flapwise alternating load spectra are shown in Figure 9. It is clear that the stable atmosphere case with the turbulent burst induces a greater number of higher amplitude cycles in the flap bending moment, including the 560-kNm cycle discussed above.

The differences in inflow and accompanying turbine responses for the daytime and nocturnal cases are not surprising given the discrepancies noted previously in the velocity and Reynolds stress components shown in Figures 4 and 5. A clue to what is happening with the intense event contained in the nocturnal case can be seen by examining the vertical flux of turbulent kinetic energy plotted for the 15-, 37-, and 58-m heights in Figure 10. Here the 200-second segment in the vicinity of the event shows a very strong downward flux (*w'e*) of high levels of TKE at the 58-m level into the layer occupied by the turbine rotor disk. It also shows that this energy is being increasingly damped as it reaches the hub of the turbine (37 m) and the lowest rotor elevation (15 m) because of increasing stability closer to the ground. The plots of Figure 10 demonstrate that the source of this coherent turbulent energy was above the rotor, possibly arising from the breakdown of nocturnal atmospheric wave phenomena associated with a low-

Table 2. Turbine IMU Measurements Extreme Statistics for Both Cases

	IMU Roll Angle Rate (deg/s)	IMU Pitch Angle Rate (deg/s)	IMU Yaw Angle Rate (deg/s)	IMU X Displacement (mm)	IMU Y Displacement (mm)	IMU Z Displacement (mm)
Nocturnal	0.71	2.14	2.22	0.26	0.24	0.20
Maximum	0.48	1.32	1.34	0.21	0.13	0.15
Values	0.81	1.53	1.61	0.20	0.20	0.14
Daytime	0.35	0.73	1.02	0.11	0.11	0.08
Maximum	0.37	0.79	1.04	0.13	0.12	0.07
Values	0.56	0.99	1.47	0.14	0.14	0.10
Nocturnal	-0.65	-1.97	-1.91	-0.28	-0.21	-0.23
Minimum	-0.46	-1.44	-1.29	-0.21	-0.14	-0.15
Values	-0.50	-1.35	-1.54	-0.20	-0.17	-0.14
Daytime	-0.38	-0.72	-1.06	-0.14	-0.11	-0.09
Minimum	-0.38	-0.81	-1.01	-0.13	-0.12	-0.09
Values	-0.40	-0.88	-1.33	-0.14	-0.13	-0.09

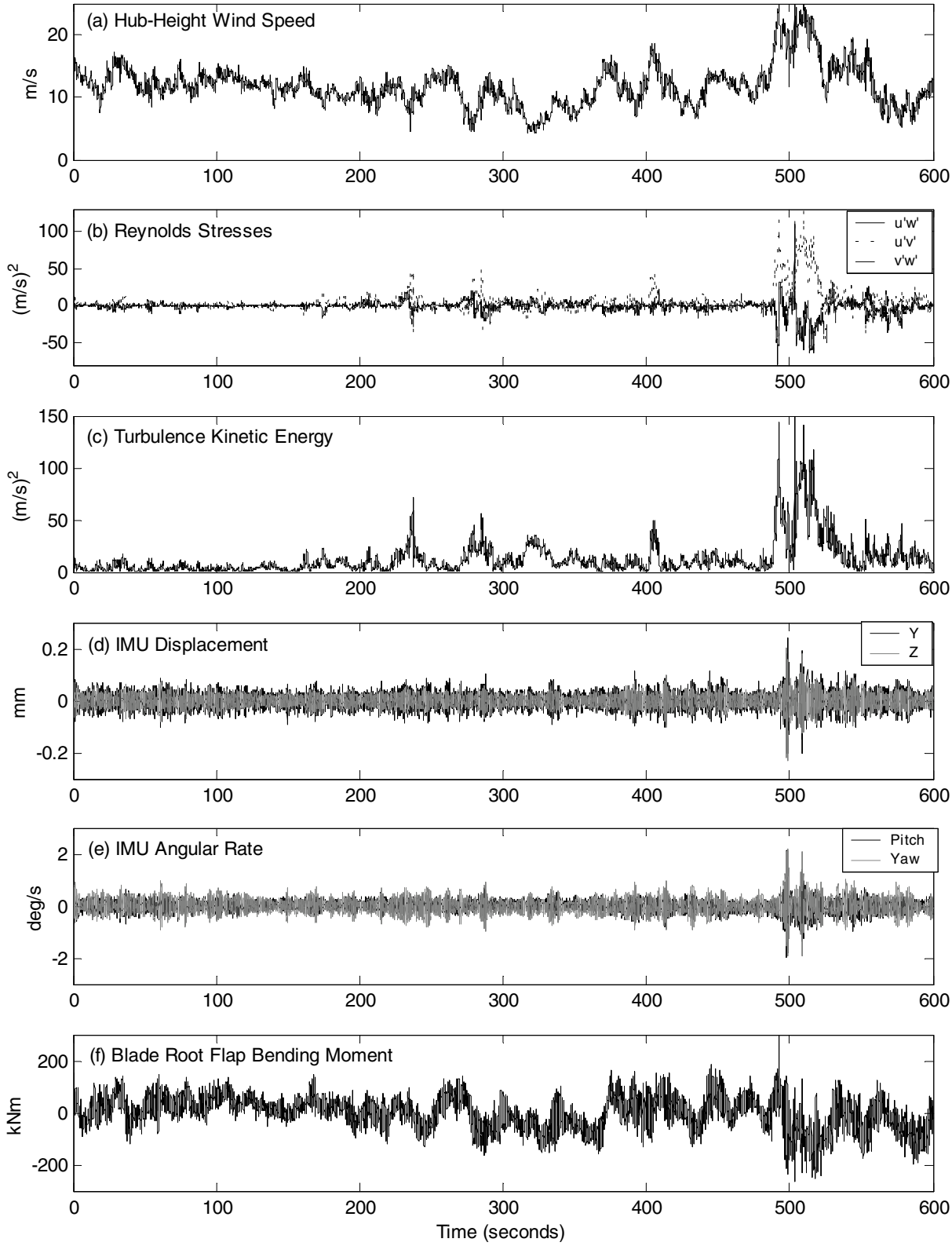

Figure 7. Ten-minute record of inflow and turbine time-series responses for nocturnal boundary layer example case

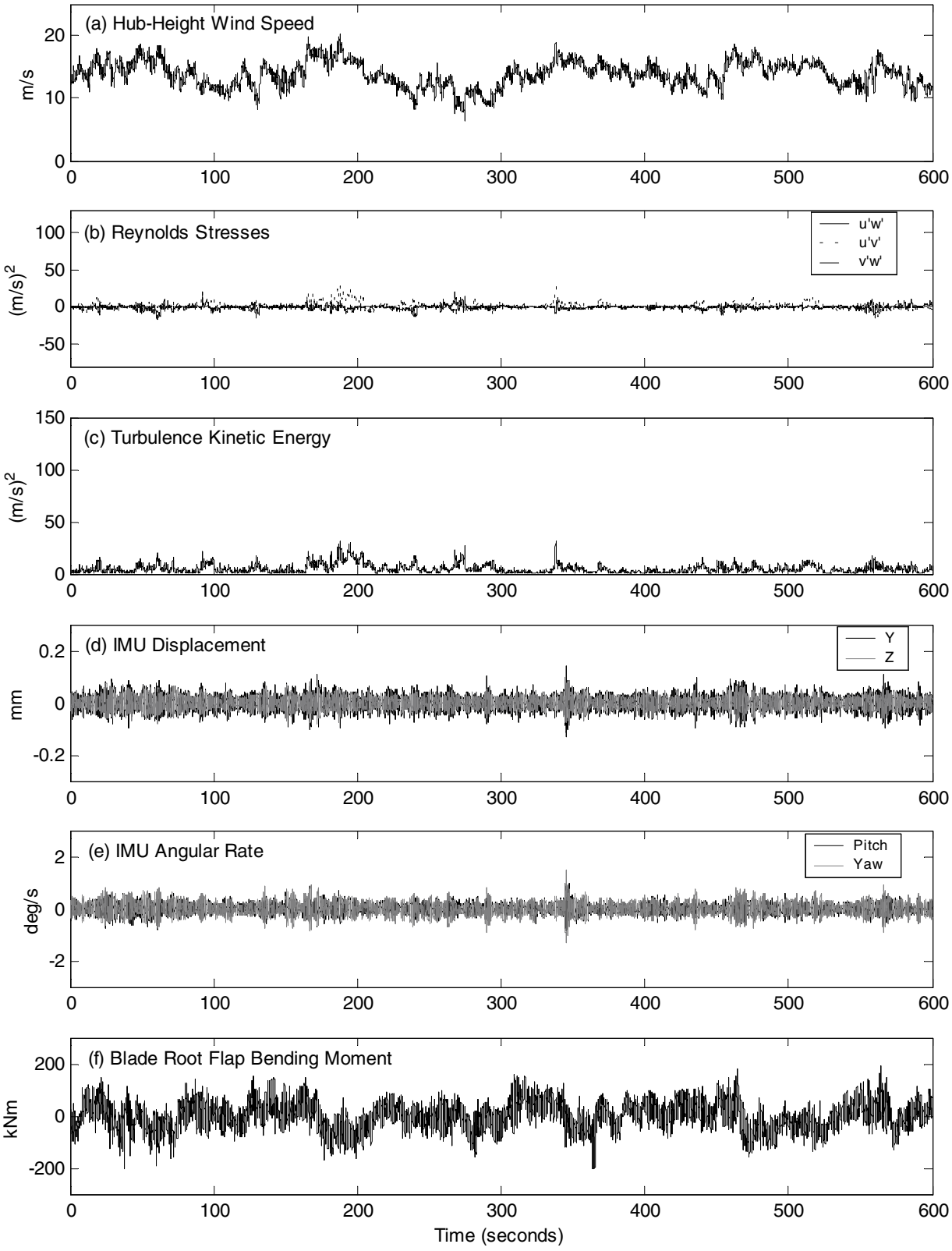

Figure 8. Ten-minute record of inflow and turbine time-series responses for daytime boundary layer example case

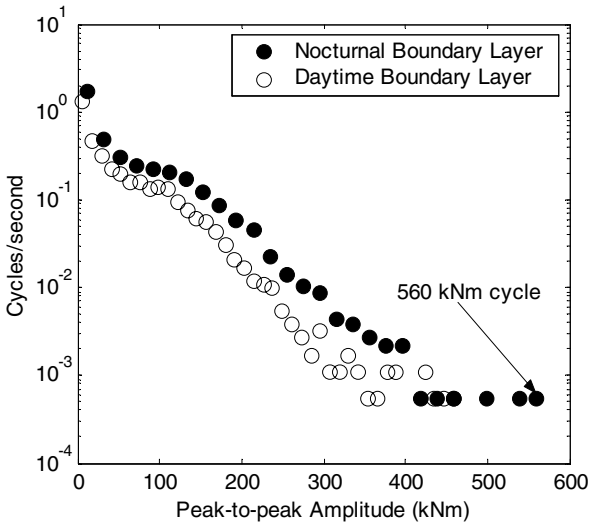

Figure 9. Comparison of blade alternating root flapwise loading spectra for daytime and nocturnal boundary layer example cases

level jet stream above the NWTC similar to those found by Banta et al.[11]

The failure of the turbulence models to simulate this extreme Reynolds stress event suggests that phenomena not included in the models are occurring in the nocturnal stable case. Further, this case demonstrates the failure of surface layer scaling because the source of the intense turbulence is not associated with surface roughness features but turbulence generating mechanisms located in the mixed layer above. In fact, most of the rotor disk is not within the surface layer for the nocturnal, stable case, as it is for the daytime, unstable case. This is demonstrated by the contents of Table 3. In the unstable case, the vertical variation of the mean Reynolds stress component $\overline{u'w'}$ is constant in the lower elevations and the mean vertical TKE flux is

Table 3. Turbulent Stress and TKE Vertical Flux Variation with Height Above Ground

	Daytime (unstable)		Nocturnal (stable)	
Height (m)	$\overline{u'w'}$ $(m/s)^2$	Mean Vertical TKE Flux $(m/s)^3$	$\overline{u'w'}$ $(m/s)^2$	Mean Vertical TKE Flux $(m/s)^3$
58 (Upper)	-0.242	0.165	-1.851	-5.234
37 (hub)	-0.534	0.240	-1.238	-2.994
15 (Lower)	-0.539	0.227	-0.616	-0.965

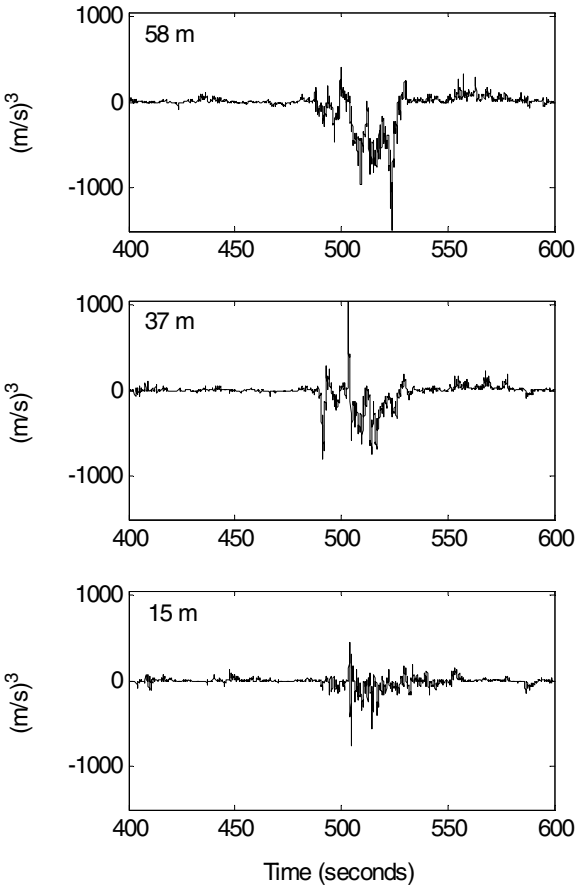

Figure 10. Detail of time-series of vertical TKE flux at 15-, 37-, and 58-m elevations for the nocturnal boundary layer example case

positive, signifying the presence of a surface layer. However, in the nocturnal case, the mean stress increases with height and is associated with the negative flux or downward transport of TKE from above. These properties do not conform to the definition of a surface layer, and therefore the turbulence scaling necessary for this situation cannot be accommodated with currently available inflow turbulence simulation codes. Marht[15] has dubbed this situation as the "upside-down" boundary layer where he notes that the primary turbulence generation mechanisms are elevated and not due to the effects of surface friction. Thus new mixed-layer scaling relationships will need to be developed in order to adequately simulate the inflow turbulence conditions associated with important loading events, such as have been demonstrated here.

CONCLUSIONS

Current stochastic inflow turbulence simulators generate planar turbulence fields that are reasonably representative of conditions that exist in the unstable

surface layer region of the planetary boundary layer. However, as turbine rotors reach higher into the PBL, this may no longer be true. We have presented limited evidence that even at moderate heights, the current simulation codes do not adequately reproduce the intermittent bursts of intense, organized turbulence that frequently occur in the nocturnal boundary layer. As was demonstrated by wavelet analysis in Kelley et al.[10] and in our stable flow example, these turbulent bursts have the potential to induce significant loading events on wind turbine structures. This situation is expected to worsen as turbine rotors continue to reach deeper into regions of the stable, nocturnal boundary layer that support phenomena such as low-level jet streams, which are responsible for generating intense coherent turbulent motions beneath them. How much worse will depend on the rate of occurrence of these motions in a specific location, something currently we do not know.

We have demonstrated, with these two examples, that turbulence-scaling relationships employed with the present turbulence simulation codes do not adequately generate the flow conditions seen in the stable, nocturnal boundary layer above 30 m (~100 ft). Even in unstable, daytime conditions at higher elevations, the upper limits to which surface-layer scaling can be applied acceptably for wind turbine operations is not presently known.

FUTURE WORK

The NWTC LIST data set will be used to examine the properties of the flow entering the turbine rotor disk. We intend to establish the percentage of time all or parts of the rotor disk are located within the surface and mixed layers in order to ascertain how important an inflow simulation of the mixed layer would be for analyzing the structural and fatigue performance of a turbine the size and height of the NWTC ART. We also will establish if it is feasible to suitably modify the existing stochastic turbulence simulators to generate turbulent structures characteristic of heights at which turbines operate in the mixed layer, in particular the nocturnal mixed layer, or if simulations based directly on the fundamental equations of motion will be required.

We plan to perform a systematic analysis of the available NWTC LIST data set in which the extent of the scaling discrepancies exemplified in this paper will be documented. From the available atmospheric information, we plan to examine new turbulence-scaling relationships that may be applied for flows of interest to wind turbine operations; i.e., wind speeds for both operating and parked turbines. We hope to expand these results as measurements at heights above those measured in the NWTC LIST Program become available. We also wish to more quantitatively establish the impact specific properties of the flow have on the fatigue life of turbine components and operational reliability.

ACKNOWLEDGMENTS

This work could not have been completed without the extensive support we received from our NREL colleagues, subcontractors, and consultants. The authors wish to thank Mike Robinson for his vision and support in establishing this program. We thank Dave Simms for his management support of the ART facility. We are indebted to Lee Jay Fingersh and Dave Jager for providing us with the PCM turbine data acquisition system on such short notice. Without the support of Jim Adams and our Mountain Valley Energy colleagues (Robert Keller, Todd Longacre, Doug Cook, Grant McFarland, and William Kimbrough), we would not have had the superb inflow array and site infrastructure. We appreciate the excellent turbine operations, maintenance, and instrumentation support afforded us by Scott Wilde and our World Power colleagues, Garth Johnson and Andy Meiser, who were always available to solve problems. We salute the efforts of our Martin/Martin consulting engineers, Jack Petersen and Russ Leffler, for their successful designs to minimize the contamination of sonic anemometer measurements from the support boom motions. We thank our NREL Information Systems colleague, Jim Mittl, for his significant contribution to the success of the inflow data system. Finally, but definitely not least, we thank M.C. “Buddy” Haun of Emergent Information Technologies, Inc., who took on the very difficult job of developing the successful LabView®-based data acquisition system for the inflow array.

REFERENCES

[1]Veers, P.S., *Three-Dimensional Wind Simulation,* SAND88-0152, Albuquerque, NM: Sandia National Laboratories, March 1988.

[2]Kelley, N.D., “The Identification of Inflow Dynamics Parameters That Can Be Used to Scale Fatigue Loading Spectra of Wind Turbine Structural Components,” NREL/TP-442-6008, Golden, CO: National Renewable Energy Laboratory, 1994.

[3]Kelley, N.D., "Turbulence Descriptors for Scaling Fatigue Loading Spectra of Wind Turbine Structural Components," NREL/TP-442-7035, Golden, CO: National Renewable Energy Laboratory, 1994.

[4]Kelley, N.D., "A Case for Including Atmospheric Thermodynamic Variables in Wind Turbine Fatigue Loading Parameter Identification," NREL/CP-500-26829, Golden, CO: National Renewable Energy Laboratory, 1999.

[5]Sutherland, H.J., and Kelley, N.D., "Fatigue Damage Estimate Comparisons for Northern European and U.S. Wind Farm Loading Environments," *WindPower '95. Proc. Of the Annual Conference and Exhibition of the American Wind Energy Assoc.*, Washington, DC: American Wind Energy Association, 1995.

[6]Kelley, N.D., "Full Vector (3-D) Inflow Simulation in Natural and Wind Farm Environments Using an Expanded Version of the SNLWIND (Veers) Turbulence Code," NREL/TP-442-5225, Golden, CO: National Renewable Energy Laboratory, 1993.

[7]Kelley, N.D., Wright, A.D., Buhl, M.L., and Tangler, J.L., " Long-Term Simulation of Turbulence-Induced Loads Using the SNLWIND-3D, FAST, YawDyn, and ADAMS Numerical Codes," NREL/CP-4400-21673, Golden, CO: National Renewable Energy Laboratory, 1996.

[8]Kelley, N.D., and Sutherland, H.J., "Damage Estimates from Long-Term Structural Analysis of a Wind Turbine in a U.S. Wind Farm Environment," NREL/CP-440-21672, Golden, CO: National Renewable Energy Laboratory, 1997.

[9]Kelley, N.D., Wright, A.D., and Osgood, R.M., "A Progress Report on the Characterization and Modeling of a Very Flexible Turbine Design," NREL/CP-500-25513, Golden, CO: National Renewable Energy Laboratory, 1998.

[10]Kelley, N.D., Osgood, R.M., Bialasiewicz, J.T., and Jakubowski, A., "Using Wavelet Analysis to Assess Turbulence/Rotor Interactions," *Wind Energy*, Vol. 3, London: John Wiley & Sons, Ltd., p. 121-134, 2000.

[11]Banta, R.M., Olivier, L.D., Neff, W.D., Levinson, D.H., and Ruffieux, D., "Influence of Canyon-Induced Flows on Flow and Dispersion over Adjacent Plains," *Theoretical Applied Climatology*, Vol. 52, p. 27-42, 1995.

[12]Petersen, J.E., Martin/Martin Consulting Engineers, *Personal communications.*

[13]Haun, M.C., Kelley, N.D., and McKenna, H.E., "Increasing Turbine System Flexibility with NI LabVIEW," *Instrumentation Newsletter,* Vol. 13, No.2, National Instruments Corp., p. 12, 2001.

[14]Simms, D., "NREL Unsteady Aero Experiment: Aerodynamic Pressure Measurements from a Rotating S809 Airfoil on a 10m Diameter 3-Bladed Downwind HAWT." McAnulty, K.F., ed. IEA R&D WECS Experts Meeting: Proceedings of the Sixth IEA Symposium on the Aerodynamics of Wind Turbines, 30 November - 1 December 1992, Petten, The Netherlands. United Kingdom: Harwell; 16 pp., 1993.

[15]Marht, L., "Stratified Atmospheric Boundary Layers," *Boundary-Layer Meteorology*, Vol. 90, p. 375-396, 1999.

REPORT DOCUMENTATION PAGE

Form Approved
OMB NO. 0704-0188

1. AGENCY USE ONLY (Leave blank)	2. REPORT DATE	3. REPORT TYPE AND DATES COVERED
	February 2002	Conference Paper

4. TITLE AND SUBTITLE
The NREL Large-Scale Turbine Inflow and Response Experiment – Preliminary Results

5. FUNDING NUMBERS
WER11020

6. AUTHOR(S)
Neil Kelley, Maureen Hand, Scott Larwood, Ed McKenna

7. PERFORMING ORGANIZATION NAME(S) AND ADDRESS(ES)

8. PERFORMING ORGANIZATION REPORT NUMBER

9. SPONSORING/MONITORING AGENCY NAME(S) AND ADDRESS(ES)
National Renewable Energy Laboratory
1617 Cole Blvd.
Golden, CO 80401-3393

10. SPONSORING/MONITORING AGENCY REPORT NUMBER
NREL/CP-500-30917

11. SUPPLEMENTARY NOTES

12a. DISTRIBUTION/AVAILABILITY STATEMENT
National Technical Information Service
U.S. Department of Commerce
5285 Port Royal Road
Springfield, VA 22161

12b. DISTRIBUTION CODE

13. ABSTRACT *(Maximum 200 words)*

The object of the experiment described in this paper is to obtain simultaneously collected turbulence information from the inflow array and the corresponding structural response of the turbine. This overview provides examples of two cases of inflow characteristics and turbine response collected under daytime and nighttime conditions and compare their turbulence properties with predictions.

14. SUBJECT TERMS
wind turbine; turbine response; energy production; wind energy

15. NUMBER OF PAGES

16. PRICE CODE

17. SECURITY CLASSIFICATION OF REPORT	18. SECURITY CLASSIFICATION OF THIS PAGE	19. SECURITY CLASSIFICATION OF ABSTRACT	20. LIMITATION OF ABSTRACT
Unclassified	Unclassified	Unclassified	UL

NSN 7540-01-280-5500

Standard Form 298 (Rev. 2-89)
Prescribed by ANSI Std. Z39-18
298-102